



UNIVERSITY OF LEEDS

This is a repository copy of *Comparison of central and end spark position for gas explosion vessels with L/D of 2.8 and 2.0*.

White Rose Research Online URL for this paper:  
<http://eprints.whiterose.ac.uk/105085/>

Version: Accepted Version

---

**Proceedings Paper:**

Fakandu, BM, Andrews, GE and Phylaktou, HN (2014) Comparison of central and end spark position for gas explosion vessels with L/D of 2.8 and 2.0. In: Proceedings. Tenth International Symposium on Hazard, Prevention and Mitigation of Industrial Explosions (X ISHPMIE), 10-14 Jun 2014, Bergen, Norway. . ISBN 978-82-999683-0-0

---

**Reuse**

Unless indicated otherwise, fulltext items are protected by copyright with all rights reserved. The copyright exception in section 29 of the Copyright, Designs and Patents Act 1988 allows the making of a single copy solely for the purpose of non-commercial research or private study within the limits of fair dealing. The publisher or other rights-holder may allow further reproduction and re-use of this version - refer to the White Rose Research Online record for this item. Where records identify the publisher as the copyright holder, users can verify any specific terms of use on the publisher's website.

**Takedown**

If you consider content in White Rose Research Online to be in breach of UK law, please notify us by emailing [eprints@whiterose.ac.uk](mailto:eprints@whiterose.ac.uk) including the URL of the record and the reason for the withdrawal request.



[eprints@whiterose.ac.uk](mailto:eprints@whiterose.ac.uk)  
<https://eprints.whiterose.ac.uk/>

# Comparison of central and end spark position for gas explosions in vessels with L/D of 2.8 and 2.0

Bala M. Fakandu, Gordon E. Andrews and Herodotos N. Phylaktou

E-mail: profgeandrews@hotmail.com

School of Chemical and Process Engineering

University of Leeds, LS2 9JT, UK.

## Abstract

Current explosion vent design correlations and guidance are based on an experimental data base of centrally ignited vented tests. However, there is evidence in the literature that ignition positions other than central produce higher overpressures. The objective of this work was to compare central and end ignition of vented explosions in a 10L and a 200L cylindrical vessels of L/D of 2.8 and 2 respectively, with vent area coefficients of 10.9, 5.4 and 3.1 for free venting. Methane-air (10% v/v) and ethylene-air (7.5%) explosion tests were carried out using a 16J spark ignition at the far end wall opposite the vent and half way along the length of the vessel. The results showed that for both vessels and for both gas/air mixtures end ignition produced the highest overpressures. This was attributed to the higher axial flame speed towards the vent with far end ignition, inducing higher vent mass flows and higher external flame speeds and associated overpressures. The present results and other data from the literature show that the vent design guides may not be based on sufficiently conservative data and need to be reviewed.

Keywords: Explosion venting, ignition location, explosion overpressure.

## 1. Introduction

The principle of explosion venting is to reduce the peak explosion overpressure,  $P_{red}$ , so as to minimise the resulting damage, by providing sufficient vent area,  $A_v$ , that opens early enough to release the explosion pressure successfully. Experimental evidence has shown that the resulting explosion overpressures are controlled by different physical mechanisms depending on the vent design and the vessel volume,  $V$  (Nagy and Verikas, 1983; Cooper et al.; 1986, Bauwen et al, 2010; Fakandu et al. 2013). The spark position for the worst case overpressure is not addressed in current design procedures or explosion venting models, as all assume that central ignition is the worst case and are based on experiments in vented explosions with central ignition (NFPA, 2013, Bradley and Mitcheson, 1978, Molkov, 2000, Cooper et al, 1986). Nagy and Verakis (1983) showed, for a rectangular enclosure with an  $L/D = 1.4$  and a square cross section, that the peak explosion overpressure increased as the spark was moved away from the vent towards the wall opposite the vent. However, this was carried out for a very small vent area,  $A_v$ , with a  $K_v = V^{2/3}/A_v$  and the present work was carried out to investigate this phenomena at more realistic values of  $K_v$ . Also the literature on the influence of spark position on  $P_{red}$ , reviewed below is confusing with contradictory findings.

## 2. Review of the influence of ignition position on vented explosion overpressure

The ATEX directive requires that for the design of safety systems the worst possible scenario must be considered (European Parliament and Council, 1994). It should be noted that for compact vented vessels with L/D close to 1, central ignition has been assumed to have the highest overpressure, in spite of the work of Nagy and Verakis (1983) showing that this was not the case. More recently Sato et al. (2010) have shown that ignition closer to the vent and away from the centreline of the vessel have higher  $P_{red}$  than for central ignition. Ignition at the vent outlet can in some circumstances be the worst case (Bauwens et al., 2010). This was found in a  $64\text{m}^3$  vessel and was shown to be higher for front and central ignition as compared to end ignition and was due to the pressure oscillations caused by acoustic interactions,  $P_{ac}$ , at the end of the explosion. Cooper et al (1986) showed that  $P_{ac}$  was not significant for practical application, as it could be eliminated using an acoustic absorber (Cooper et al, 1986). As Bauwens et al. (2010) used a relatively thin walled vessel this oscillatory pressure peak was also likely to be an artifact of vessel wall resonance. In the present work with thick walled vessel no acoustic pressure peak was found. Bauwens et al. (2010) concluded that which ignition position (end, central or vent outlet) is the worst case depends on the mixture and the vent coefficient.

In experiments carried out by Cabbage and Simmond (1955) for the design of explosion reliefs in industrial drying ovens central ignition was shown to be the worst case, as compared to positions away from the centre (Cabbage and Simmonds, 1955). The actual position of the various ignition positions and vent panels relative to the shelves were not specified, hence cannot be used as a yardstick for considering the central position as the worst case.

Other data in the literature also shows lower overpressure for end ignition as compared to central ignition (Maisey, 1965, Burgoyne and Newitt, 1955, Haris and Briscoe, 1967). Solberg et al (1981) showed for a  $35\text{m}^3$  cubic vessel that the front and central ignition gave higher overpressures compared to end ignition opposite the vent and they attributed this to Taylor instabilities. The vent position was off centre (bottom) and so there was no direct acceleration path from the ignitor to the vent and this may have prevented the fast flame development that is seen with wall ignition opposite the vent. Most of the researchers that found higher overpressure for central ignition argued that for the end ignition, the flame contacted the vessel wall before reaching the vent thereby cooling the flame earlier, as compared to central ignition which did not contact the wall before emerging from the vent. This reasoning may be based on spherical flame theory rather than experimental verification. Fakandu et al. (2011) showed for the present  $0.1\text{m}^3$  cylindrical vessel that the flame touched the wall of the vessel well after the flame had exited the vent.

Willacy et al. (2007) showed, for a L/D of 2, using a  $0.2\text{m}^3$  cylindrical vented vessel explosions with a high  $K_v$  of 16.4 and a vent pipe, that ignition on the wall opposite the vent had a much higher overpressure than for central ignition. Similar work on methane-air explosion venting through a vent pipe showed that a more intense burning rate was expected for rear ignition as compared to central ignition with much higher overpressures (Ferrara et al, 2008). However, Ferrara et al (2008) were of the opinion for venting with a vent pipe that central ignition gives higher overpressure as compared to rear ignition for propane-air mixture, even though the rear ignition has a higher burning rate compared with the central ignition location. This was in agreement with other works in the literature in favour of the central ignition as the worst case overpressure for venting with a vent pipe attached (Ferrara et al, 2006, Ponizy and Layer, 1999a).

The work of Palmer and Rogowski (1966) found that the worst case explosion overpressure was for end ignition even though the vessel was similar in shape to that of Cubbage and Simmonds (1960). Hence, there is a need to have closer look at the effect of ignition position on explosion venting and in this work in a cylindrical configuration ignition at the end wall opposite the vent was compared with central ignition. This follows the finding of Nagy and Verakis (1983) that  $P_{red}$  increased as the spark was moved further away from the vent on the vent centreline. A spark on the end wall is thus the worst case according to their findings, which are in agreement with those of Palmer and Rogowski (1966) but contradict many other investigations, as discussed above.

In NFPA 68 (2013) in the discussion of the determination of the vessel L/D it is assumed that for a vent on the wall of the vessel that the worst case ignition position is that furthest from the vent and that the distance of this to the vent should be used in determining the L/D. This is recognition in a design standard that ignition furthest from the vent is the worst case. Cates and Samuels (1991) also showed that the farthest location away from the vent produced the highest overpressure, even in the presence of obstacles.

### **3. Central ignition experimental results are the basis of vent design methodology.**

Most of the experimental explosion venting data is for central ignition, including the vent European venting standard and the NFPA (NFPA, 2013, BS EN 1449, 2007). This was also the assumption used by Bradley and Mitcheson (1978), Molkov (2000) as well as in the work of Bartknecht, on which the European venting standard (BS EN 14491:2007) is based. Similarly, the data used by Swift (1989) to generate his vent design equation was for central ignition and is the basis for the correlation used in the new NFPA (2013) vent design guide for gas explosion deflagration venting.

For a totally closed vessel (no vents) explosion, the central ignition location is the worst case, since the flame propagates at relatively constant speed and the flame will develop to its maximum possible surface area just before touching the walls. For any other ignition position in a spherical vessel the flame will touch the walls before all the mixture has been burned and there will then be heat losses from the burned gas to the wall which will reduce the peak pressure. However, this is not the case with end ignition in a vented explosion, as the flame accelerates towards the vent and ignition at the furthest point from the vent gives the greatest flame acceleration distance and the rate of propagation of the flame is much higher than that for a laminar spherical flame (Fakandu et al., 2011).

The flame in most vented explosions with end ignition has emerged from the vent before the flame spreads to the walls of the vessel, as will be shown in the present work. The worst case scenario should be used in order to meet the requirement of the ATEX directive and ignition with the maximum overpressure must always be considered in this regard. The aim of this work was to investigate whether end ignition was the worst case for vented explosions with ignition on the centre line of the vent.

### **4. Experimental equipment**

Two different cylindrical vessels, of 10 litres volume ( $0.010\text{m}^3$ ,  $L=0.460\text{m}$ ,  $D=0.162\text{m}$ ) shown in Figure 1 and 200 Litres ( $0.2\text{m}^3$ ,  $L=1\text{m}$ ,  $D=0.5\text{m}$ ) shown in Figure 2, were used for vented gas explosion with free venting (open vents). Different vent areas were introduced using a removable vent at the end wall attached to a 0.5m cylindrical vessel which was also connected to a large dump vessel. The L/D of the vessels were close to the limit of application of the vent design procedures for compact vessels, where the L/D of a compact vessel was  $<2$  according to the work of Bartknecht (1993) and  $<2.5$  in NFPA 68 (2013) and  $<3$  in the EU

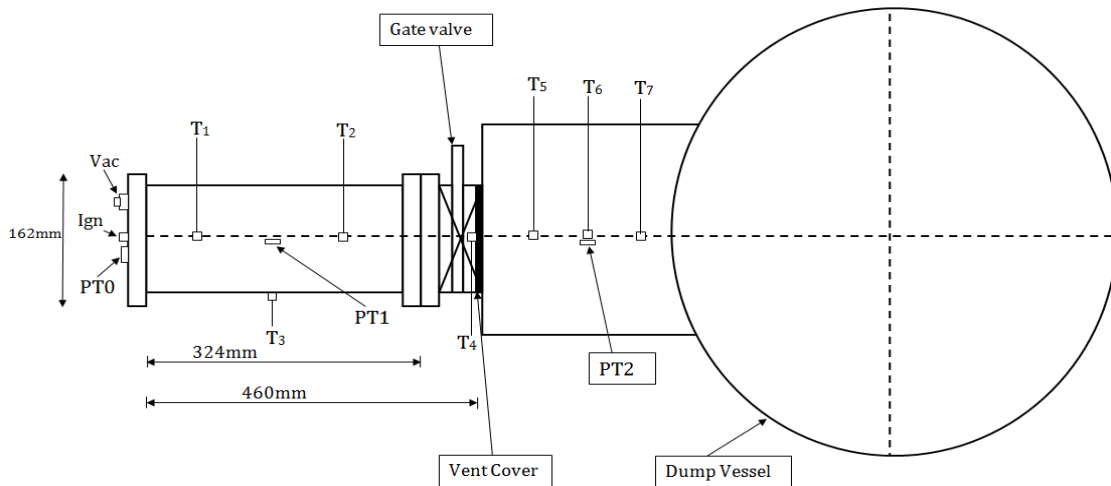


Figure 1: The 10Litre Vessel and the connecting.

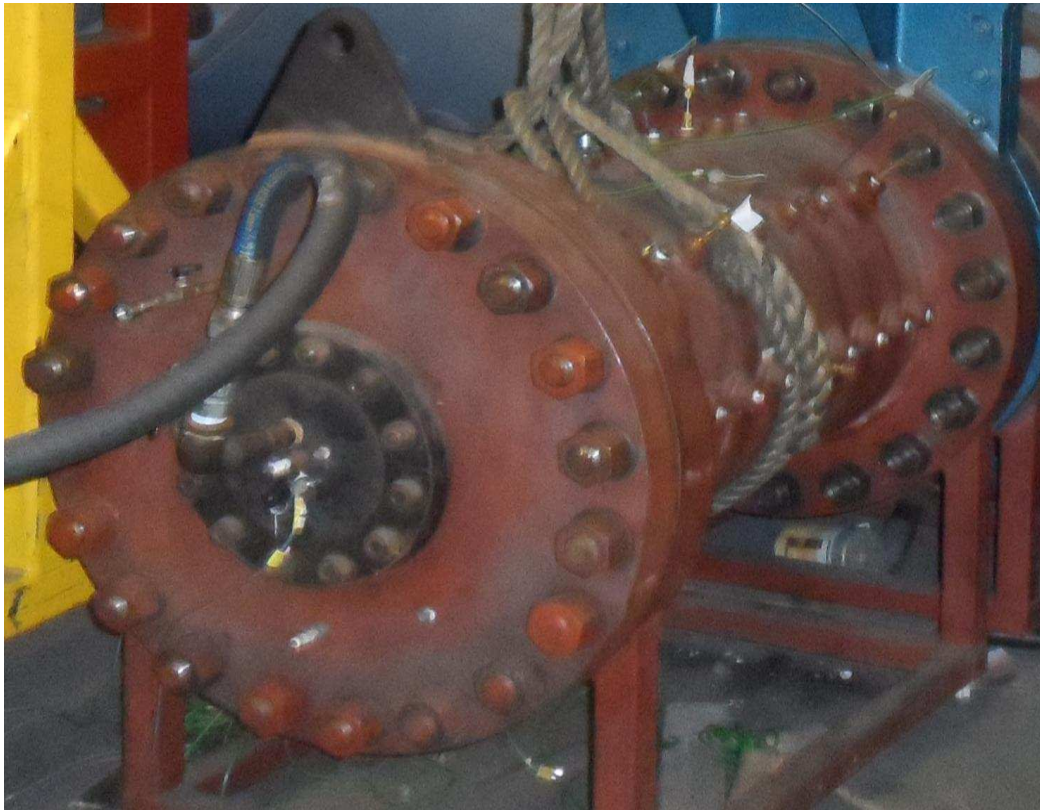


Figure 2: The 200L (0.2m<sup>3</sup>) vented vessel.

vent design guidance. The small 10L vessel was an L/D of 2.8 and the larger 200L vessel was an L/D of 2. As vessels longer than these compact vessel limits have higher  $P_{red}$  for the same volume and  $K_v$ , it is likely that vessels with  $L/D > 1$  and  $< 2$  or  $3$  will have higher overpressures than vessels that are cubic or cylinders with  $L/D = 1$ . Thus, the use of end ignition in a vessel with  $L/D = 2$  or  $2.8$  is likely to have the greatest influence of the spark location and also be the worst case for ATEX compliance.

The test vessels were connected to a 0.5m diameter cylindrical vessel which was also connected to a 50m<sup>3</sup> dump vessel, to safely capture the vented flames and which acted as a free vent condition as the dump volume was >100 times the vented volume. The 0.5m diameter vessel between the vented vessel and the dump vessel was used to mount three thermocouples on the centreline of the discharge jet so that the vented external jet flame speed could be determined as a function of distance from the vent. The ignition position was on the centreline of the end wall opposite the vent and central ignition was midway along the length of the vessel.

The flammable mixture was made up using partial pressures, starting with a vacuum in the explosion vessel. Piezo resistive pressure transducers were mounted in the end flange on which the spark plug was mounted and a second pressure transducer was mounted on the centreline of the vessel cylindrical wall. A 32 channel 100 kHz per channel data logging system was used to record all the data.

The flame travel time was recorded by mineral insulated, exposed junction type-K thermocouples, arranged axially at the centre line of both vented vessels and the 0.5m diameter discharge vessel, as shown in Figure 1 for the 10L vessel, thermocouples T<sub>1</sub>, T<sub>2</sub> and T<sub>4</sub> were located on the centreline of the main test vessel with T<sub>4</sub> at the vent plane to determine when the flame exited the vent. Thermocouples T<sub>5</sub>, T<sub>6</sub> and T<sub>7</sub> were mounted on the centreline of the 0.5m dia. connecting vessel. For the larger 200L vessel, T<sub>1</sub>, T<sub>2</sub>, T<sub>4</sub>, T<sub>5</sub> and T<sub>6</sub> were thermocouples upstream of the vent and T<sub>7</sub>, T<sub>8</sub> and T<sub>9</sub> downstream. The time of flame arrival was detected from the thermocouples' start of temperature rise and the flame speed between two thermocouples was calculated and plotted as the flame speed for the midpoint between the two thermocouples. There was also another thermocouple, T<sub>3</sub>, located on the wall of the main test vessels to measure the time of flame arrival at the wall of the vessel, which was taken to be the time of maximum flame area inside the vessel. These event times are marked on the pressure time results with the thermocouple location, so that the position of the flame when a peak in the pressure time record occurs can be determined. This enabled precise determination of whether the highest overpressure was generated by an external explosion, P<sub>ext</sub>, or by the internal flame displacing unburned gas through the vent, P<sub>fv</sub>. The time of arrival at T<sub>3</sub> could be taken as the maximum flame area time and this could then identify whether this corresponded with a pressure peak, P<sub>mfa</sub>, as identified as an important pressure peak in the work of Cooper et al. (1986) and Bauwens et al. (2010).

Two piezo electric pressure transducers were used with one at the end flange (PT0) opposite the vent and mid-way the vessel length (PT1) respectively as shown in Figure 1. In low flame speed explosions these pressure transducers had identical pressure time characteristics and only pressure records for PT0 are reported in this work. For hydrogen explosions there were dynamic flame events that caused these two pressure transducers to record different pressure time records (Fakandu et al, 2011 and Fakandu et al., 2012). A third transducer PT2 was located in the 0.5m dia. connecting vessel which measured the external explosion overpressure and its time of occurrence. This was of great assistance in determining when the external explosion occurred.

## 5. Results and discussion

### 5.1 The nomenclature for physical flame phenomena that can cause a pressure peak in vented explosions.

Pressure time records for vented explosions are associated with range of events that cause the pressure to rise and fall and which of these pressure peaks is the maximum overpressure, P<sub>red</sub>,

depends on the vent design, vessel volume, mixture reactivity and ignition position. The pressures peaks have different nomenclature depending on the physical phenomenon responsible. The first pressure peak ( $P_{burst}$ ) is as a result of the opening of the vent cover at the static burst pressure  $P_{stat}$  to allow for venting. This is not applicable in this work as free venting (uncovered vent) was used. The next pressure peak that usually occurs is  $P_{fv}$  caused by the flow of unburnt gases through the vent. This is followed by  $P_{ext}$  due to the external explosion downstream of the vent. There can also be  $P_{mfa}$  due to the maximum flame area inside the vessel, which usually occurs after the external explosion. The pressure rise by the external explosion can cause a reverse flow back into the vessel causing turbulent combustion of the unburned gas mixture inside the vessel leading a pressure peak  $P_{rev}$ . This can be the peak overpressure if there is a large proportion of the initial gas mixture still unburned after the flame leaves the vent. This is more likely to be the case for central ignition or ignition closer to the vent, as shown by Nagy and Verakis (1983). Finally  $P_{ac}$  is the pressure caused by high frequency acoustic resonance. This oscillatory pressure peak was not the dominant pressure peak in any of the present vented explosions. The various pressure peaks are indicated on the pressure-time profiles in this paper using the above identification terms.

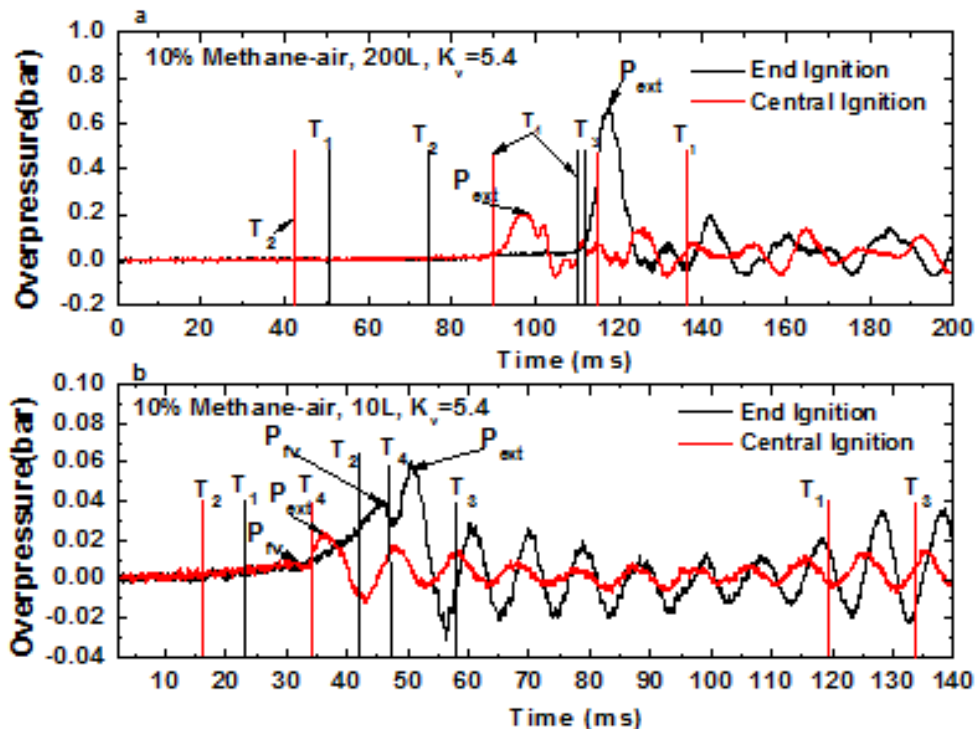


Figure 3: Comparison of central and end ignition for  $K_v = 5.4$  for 10% methane-air for (a) the  $0.2 \text{ m}^3$  vessel and (b) the  $0.01 \text{ m}^3$  vessel.

## 5.2 Influence of ignition location on explosion overpressure for low $K_v$ of 5.4 and 3.1 for 10% methane-air.

Figure 3 compares the pressure-time profile for central and end ignition with  $K_v = 5.4$  for 10% methane-air for (a) the  $0.2 \text{ m}^3$  vessel and (b) for the  $0.01 \text{ m}^3$  vessel. Figure 3 shows that the end ignition opposite the vent gave much higher overpressures compared with central ignition for both test vessels. For both cases with end and central ignition the external explosion controlled the peak overpressure as shown by the peak overpressure occurring after the flame had emerged from the vent and past thermocouple  $T_4$ . For both vessel volumes the ratio of the

end ignition  $P_{ext}$  to that for central ignition was 3.1 for the  $0.2 \text{ m}^3$  vessel and 2.7 for the  $0.01 \text{ m}^3$  vessel and it would be reasonable to take a ratio of the two peak pressures as 3.

Figure 3 shows that for central ignition the flame propagation was entirely towards the vent and this left a large volume of unburned gas behind the flame front inside the vessel. This is shown by the very long time, well after the peak pressure had been reached, for the flame to reach thermocouples  $T_2$  upstream of the spark and  $T_3$  at the wall in the plane of the spark. This time was proportionately longer in the smaller vessel than the larger vessel, indicating faster flame propagation in the larger vessel. In the larger vessel there was no discernable pressure peak due to the unburned gas flow through the vent,  $P_{fv}$ , but this was a clear peak in the smaller pressure peak. This may be because for the larger vessel the external explosion overpressure was much larger than for the smaller vessel that  $P_{fv}$  cannot be seen in the scale of Fig. 3. This paper is concerned with the influence of the ignition position and will not be discussing the reason for the higher overpressures in the larger vented vessel.

This large difference in overpressure between end and central ignition was due to the expansion of the flame in the direction of the vent with convection of the flame by the vent outflow. This effect was greater for the larger distance of the spark from the vent and results in a fast flame approaching the vent, as will be shown later. This fast flame drives unburned gases ahead of it so that the unburned gas mass flow through the vent is higher for the end vented case. This creates a greater volume of unburned gas outside the vent and a higher external explosion overpressure as a result for the end ignition case. Also as the flame velocity upstream of the vent is higher than for central ignition, there is more turbulence in the external unburned gas cloud and hence a faster external explosions and higher external overpressure.

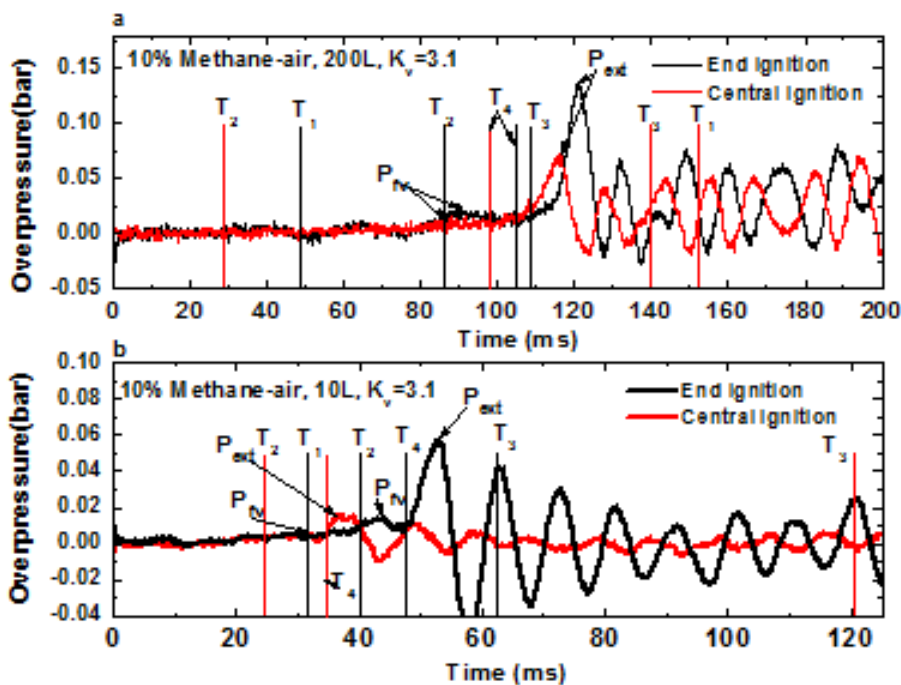


Figure 4: Comparison of central and end ignition for  $K_v = 3.1$  for 10% methane-air for (a) the  $0.2 \text{ m}^3$  vessel and (b) the  $0.01 \text{ m}^3$  vessel.



With central ignition the flame leaves the vent earlier than for end ignition with a smaller external cloud of unburned mixture. Also the flow of unburned gas through the vent is lower due to the slower upstream flame speed. This results in lower turbulence in the external unburned gas cloud and hence a lower external flame overpressure. The earlier flame arrival at the vent also marks the start of burned gas venting, which is more efficient in reducing the overpressure than unburned gas venting.

For the lower  $K_v$  of 3.1 Fig. 4 shows that the pressure due to the flow of the unburnt gas through the vent,  $P_{fv}$ , was very low and the external explosion,  $P_{ext}$ , dominated the overpressure for both vessel volumes and for both ignition positions. The ratio of  $P_{ext}$  for end to central ignition was 2 for the larger vessel with  $L/D = 2$  and 3.7 for the smaller vessel with  $L/D = 2.8$ . For the larger vessel the flame reached the wall at  $T_3$  well after the peak external pressure and reached  $T_1$  after this, as shown in Figure 4a. There was no evidence of rapid combustion of the unburned gases left in the vessel after venting with central injection. The same occurred in the smaller vented vessel, but was even slower to reach  $T_1$ . For end ignition in the larger vessel the flame reached  $T_3$  soon after it passes through the vent at  $T_4$  and before the peak external pressure. The burning of the unburned gas inside the vessel thus contributed to the peak external overpressure. However, in the smaller vessel the flame did not reach  $T_3$  until after the peak explosion pressure.

### 5.3 Influence of end and central spark location for $K_v = 5.4$ and 3.1 for 7.5% ethylene-air

For higher mixture reactivity the flame speeds in the direction of the vent will be greater and this will increase the mass flow through the vent and the turbulence in the external unburned mixture expelled out of the vent. Ferrara et al. (2008) found that for vented explosions with a vent pipe propane gave central ignition as the worst case, whereas methane explosions had a worst case with end ignition. In the present work propane had very similar end ignition results to methane with the external explosion dominating the peak overpressure and with a much larger peak external pressure than for central ignition. However, a greater test of the influence of mixture reactivity is that of 7.5% ethylene-air mixtures, and these were investigated in the  $0.01 \text{ m}^3$  explosion vessel for the low  $K_v$  of 5.4 and 3.1.

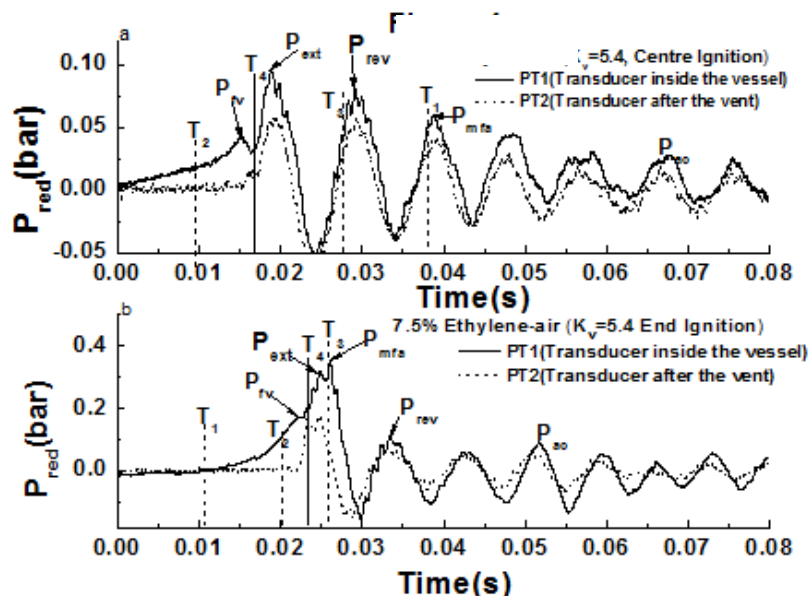


Figure 5: Comparison of (a) central and (b) end ignition for 7.5% ethylene/air vented explosions for  $K_v = 5.4$  in the  $0.01 \text{ m}^3$  vessel.

Ethylene air vented explosions were carried out with central and end ignition in the 0.01 m<sup>3</sup> explosion vessel, using the most reactive mixture of 7.5% ethylene in air. Figure 5 compares central and end ignition for pressure transducers inside and outside of the vessel. Figure 5b shows that for end ignition the peak overpressure was much higher than for central ignition by a factor of 3.9, which is greater than the factor of 3 found for methane-air explosions in Fig. 3. However, in this case neither the pressure peak due to the flow through the vent,  $P_{fv}$ , nor the external explosion overpressure,  $P_{ext}$ , was the highest overpressure. The peak overpressure occurred when the flame reached the vessel wall and was thus due to the maximum flame area,  $P_{mfa}$ , which occurred after the flame had left the vent. This maximum flame area pressure peak was only slightly higher than the external explosion overpressure but occurred after the external explosion overpressure had started to decay. This explosion also had a reverse flow pressure peak at a similar magnitude to the central ignition case, but it was nowhere near the peak overpressure.

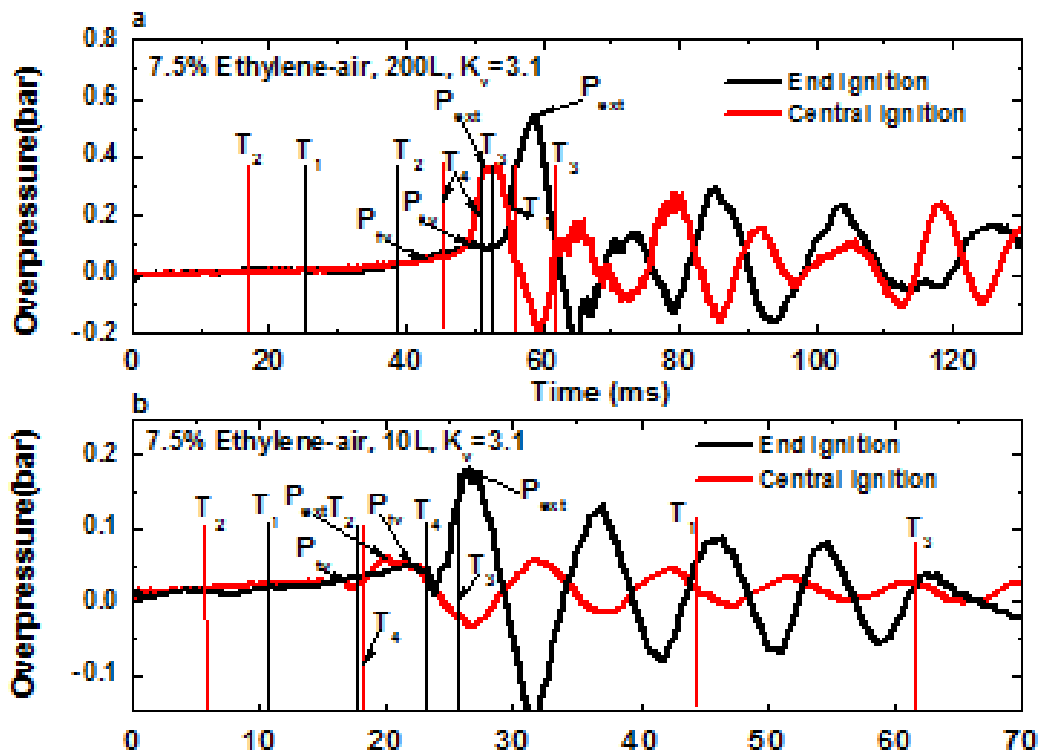


Figure 6: Pressure profiles for 7.5% Ethylene-air for  $K_v = 3.1$  with end and central ignition (a) 200L vessel (b) 10L vessel.

Central and end ignition for 7.5% ethylene/air mixtures were also compared on the 0.2 and 0.01 m<sup>3</sup> explosion vessels for  $K_v = 3.1$  and the results are shown in Figure 6. For both vessels the end ignition results gave a higher peak overpressure than for central ignition, but the difference was greater in the smaller vessel. The external explosion was also the cause of the peak overpressure for both vessel sizes. The overpressure for end ignition as a ratio of that for central ignition for 7.5% Ethylene-air for the 200L vessel was a factor of 1.5 increase. This is the smallest increase in the overpressure for end ignition in the present work. The overpressure for end ignition as a ratio of that for central ignition for 7.5% Ethylene-air for the 10L vessel was a factor of 4.3 increase. This is larger than the effect in Figures 3 and 5 for  $K_v = 5.4$ , where the difference was close to a factor of 3. This may indicate that the effect of spark location is greater for lower  $K_v$ .

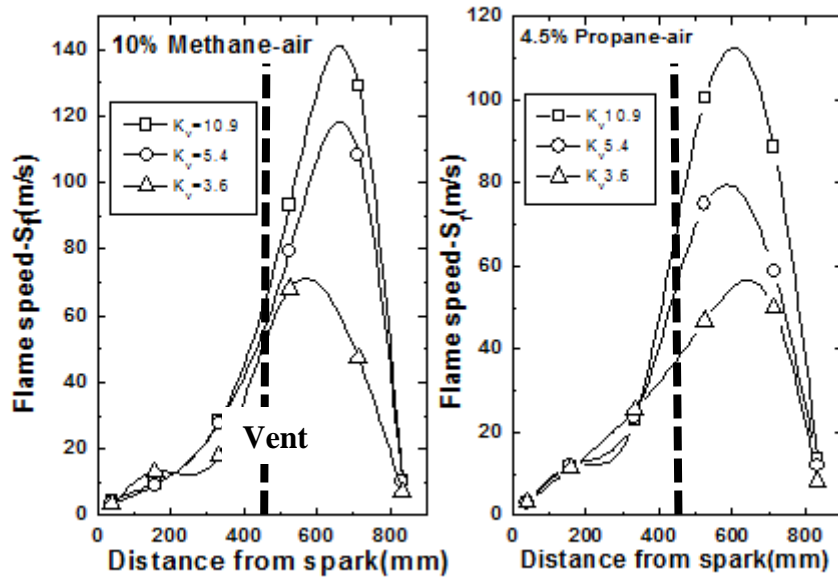


Figure 7: Flame speeds as a function of the distance from the end wall ignition through to the external flame for the  $L/D = 2.8$  vessel for  $K_v$  3.6 – 10.9

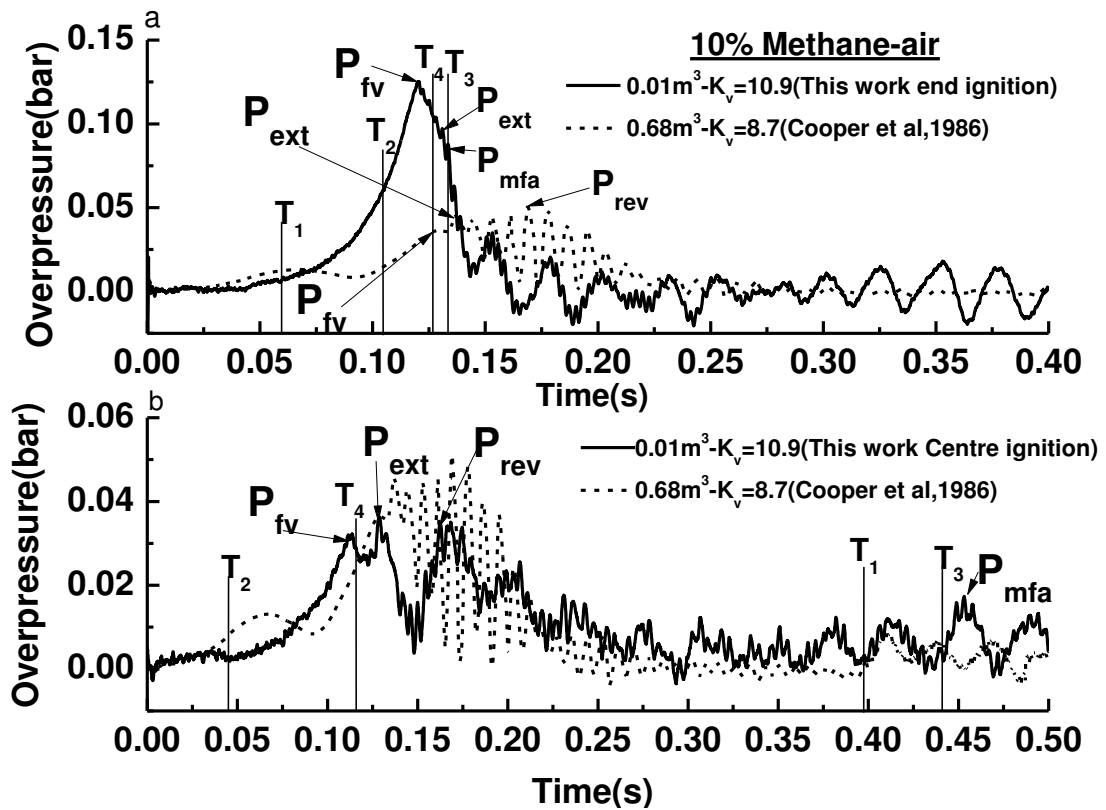


Figure 8: Pressure profiles for 10% methane-air for  $K_v = 10.9$  with end (a) and central (b) ignition, for pressure transducer PT0.

#### 5.4 Influence of central and end ignition for $K_v = 10.9$ for 10% methane-air.

Reducing the size of the vent increases the velocity through the vent for the same upstream mass burning rate and this increases the vent flow pressure peak,  $P_{fv}$ , which scales inversely with the square of the vent area (Andrews and Phylaktou, 2010). The external explosion will also be increased due to the higher vent flow velocity, which will create more turbulence in the downstream jet. However, this is a linear increase in velocity with increase in  $K_v$ , or reduction in  $A_v$ . This will produce a linear increase in the external jet turbulence and roughly a linear increase in the jet turbulent burning velocity. The external overpressure scales with the square of the external flame speed and so both the internal and external overpressure could increase in proportion and it would be difficult to predict which would dominate.

All of the above considerations rely on the assumption that the upstream flame speed and mass burning rate of the flame will be unaffected by the reduced vent outflow. Figure 7 for end ignited vented explosions for 10% methane-air and 4.5% propane air shows that increasing  $K_v$  from 3.6 to 10.9 does not change the upstream flame speed significantly, but does increase the external flame speed. However, Fig. 7 shows that the external flame speed does not increase in proportion to  $K_v$  as argued above should occur. This means that the internal vent flow overpressure,  $P_{fv}$ , is likely to rise faster than the external overpressure,  $P_{ext}$ , as  $K_v$  is increased and this is what the experimental results show. The reason for the external flame velocity not scaling with  $K_v$  is that the external flame speed is a function of the turbulent burning velocity which depends on the turbulent length scale as well as the turbulent fluctuating velocity, which should scale with  $K_v$ . As  $K_v$  is reduced the diameter of the vent is reduced and this controls the length scale and the position in the external jet at which the peak turbulence occurs.

The present  $L/D = 2.8$  and  $0.01 \text{ m}^3$  cylindrical vessel end vented results with central and end ignition for a  $K_v$  of 10.9 are compared for 10% methane-air vented explosions in Figure 8 with those of Cooper et al. (1986) for their  $L/D=3$  vessel with central ignition and a  $K_v$  of 8.7 in a  $0.68 \text{ m}^3$  rectangular volume. This difference in  $K_v$  would reduce the overpressure a little for the Cooper et al. (1986) results. To compare with comparable time scales the present results were scaled in time using  $V^{1/3}$  time scaling of the present results to the time scale for the larger volume Cooper et al. (1986) results.

For central ignition Figure 8 shows that the present pressure records were very close to those of Cooper et al. (1986) for a similar vessel  $L/D$ , but much larger volume. The present results with central ignition had a slightly lower peak pressure than found by Cooper et al. (1986). The  $P_{ext}$  external explosion was the highest overpressure and Figure 8b shows that this occurred after the flame had passed through the vent plane at time  $T_4$ , when the peak pressure due to the flow through the vent occurred,  $P_{fv}$ . This was followed by a short period of pressure reduction while the flame propagated outside the vent to reach the peak external turbulence which produced a fast flame that gave the peak overpressure,  $P_{ext}$ . These two peaks were present in the results of Cooper et al. (1986), but the flame position information was not available to determine which event caused the peak pressure, which was slightly higher than in the present work. Also, the oscillatory pressure peak,  $P_{ac}$ , was slightly higher than  $P_{ext}$  in the work of Cooper et al. (1986) as shown in Fig. 8b, but they discounted these oscillatory peaks as an artifact of using a thin metal box in the experiments. They showed that they disappeared when an acoustic absorber was used as a wall liner in the chamber. Overall the present central ignition results are in good agreement with those of Cooper et al. (1986) for a vessel with similar  $L/D$  but larger volume. This indicates that the much larger  $0.68 \text{ m}^3$  vessel volume (x70 of the present volume) of Cooper et al. (1986) has little effect on the

overpressure. In this work the distance from the spark to the vent was 0.9m compared with 0.3m in the present work for central ignition. This would indicate that self-acceleration was not significant for a spark to vent distance of at least up to 0.9m.

Figure 8a shows the end ignition results for  $K_v = 10.9$ , which have much higher overpressures than for central ignition in Figure 8b. The peak pressure was due to the flow of unburned gas through the vent, as  $P_{fv}$  occurred before the flame reached  $T_4$ . The external explosion occurred on the decaying pressure and is a slight peak on the pressure decay. The flame arrives at  $T_3$ , indicating that the maximum flame area inside the vessel occurred after the peak pressure and was not the cause of the peak pressure. The ratio of the peak pressure for end ignition to central ignition was 3.6 and this supports the results above, all of which have end to central ignition peak pressure ratios between 1.5 and 4.3. Thus end ignition had a major increase in the peak overpressure and vent design based on experiments with central ignition may not be safe designs. Current procedures based on the vented explosion results of Bartknecht (1993) are safe, in that his results are much higher than any others in the literature, even for experiments in much larger vessel than he used (Fakandu et al., 2011; Kasmani et al., 2006).

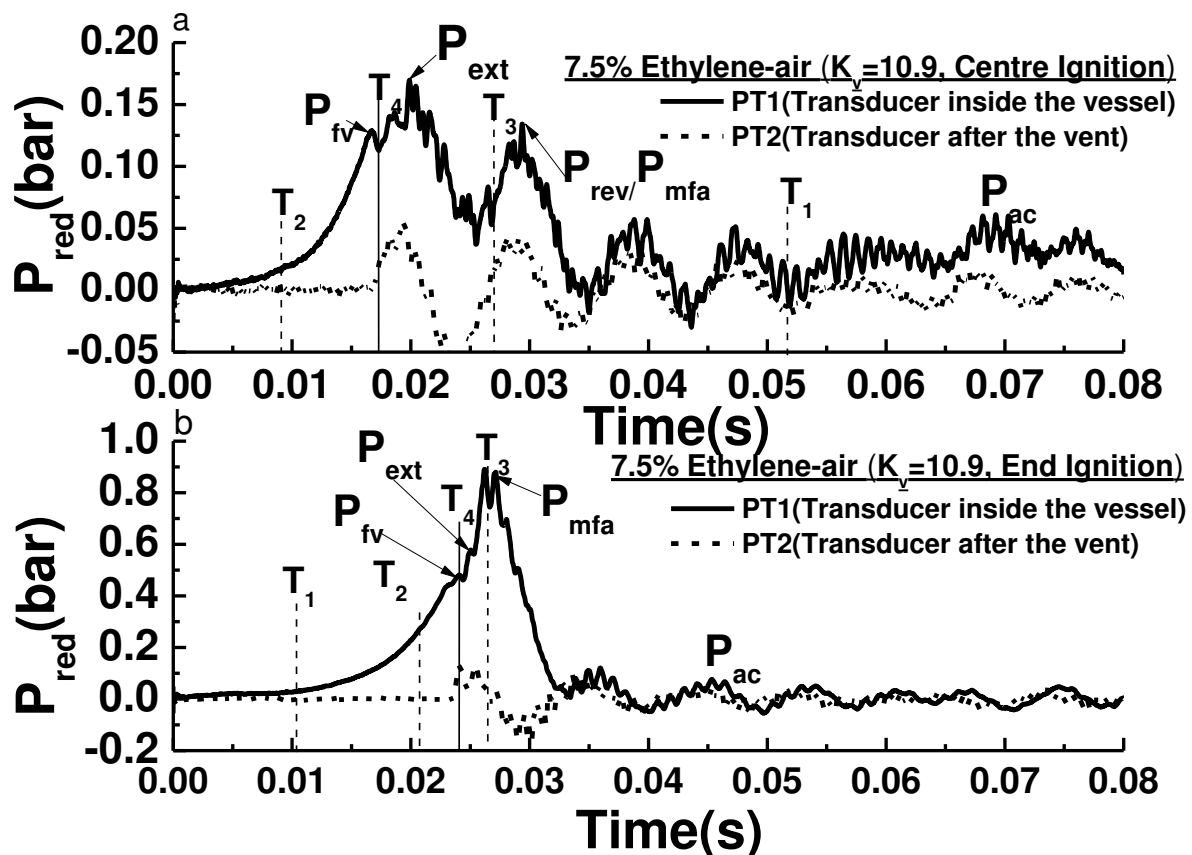


Figure 9: Pressure profiles for 7.5 % ethylene-air for  $K_v = 10.9$  with central (a) and end (b) ignition, for pressure transducer PT0 and PT2.

### 5.5 Influence of central and end ignition for $K_v = 10.9$ for 7.5% ethylene-air

Figure 9a, shows the vented explosion pressure record for the more reactive mixture with 7.5% ethylene-air and a  $K_v$  of 10.9. The external pressure transducer PT2 records are also shown. For central ignition the external overpressure  $P_{ext}$  (0.17 bar) was just higher than  $P_{fv}$

(0.16 bar). The external pressure record confirms the location of  $P_{ext}$ . The pressure peak for the maximum flame area that occurs just after  $T_3$  was quite high at 0.13 bar. Comparison to the methane results shows that for both mixtures the external explosion was the largest overpressure for central ignition. For end ignition Figure 9 shows that the external explosion  $P_{ext}$  (0.59 bar) was larger than  $P_{fv}$  (0.47 bar) but the highest overpressure was  $P_{mfa}$  (0.88 bar). This was confirmed by the external overpressure measurement aligning in time with  $P_{ext}$  and  $P_{mfa}$  aligning in time with  $T_4$  and  $T_3$  respectively. The ratio of the peak overpressure for end ignition to that for central ignition was 5.2, much higher than for methane at 3.6 at this  $K_v$ .

Figures 3-9 show that the peak overpressure can be due to any of the events ( $P_{fv}$ ,  $P_{ext}$  or  $P_{mfa}$ ), depending on  $K_v$ , gas reactivity and the ignition location. Without the present thermocouple sensors to detect the location of the flame just before a pressure peak and the use of the external pressure transducer PT2, it would be difficult to separate the cause of the various pressure peaks. However, the first two pressure peaks  $P_{fv}$  and  $P_{ext}$  are more commonly responsible for the peak overpressure. The present results for end ignition indicate that for  $K_v < \sim 5.4$   $P_{ext}$  would be the dominant overpressure and for  $K_v > \sim 5.4$   $P_{fv}$  would be dominant.

### 5.6 Influence of ignition location on flame speeds

Figure 10 shows the flame speeds for 10% Methane-air and 7.5% Ethylene-air for  $K_v=10.9$ , as a function of the ignition position. With end ignition, the flame propagated axially towards the vent and accelerated as it approached the vent, with maximum flame speed of 31m/s for 10% methane-air and 84m/s for 7.5% ethylene-air (just upstream of the vent). For 10% methane-air, the maximum flame speed of 31m/s upstream the vent was 5 times the value obtained for the centrally ignited mixtures of approximately of 6m/s and this is similar for 7.5% Ethylene-air as a factor of 4 difference in flame speeds occurred when the two ignition locations were compared, as seen in Fig. 10b. The trend of development in the upstream flame speeds, which is responsible for the maximum flame speeds obtained downstream the vents, also influences the rate of pressure rise and the final peak overpressures.

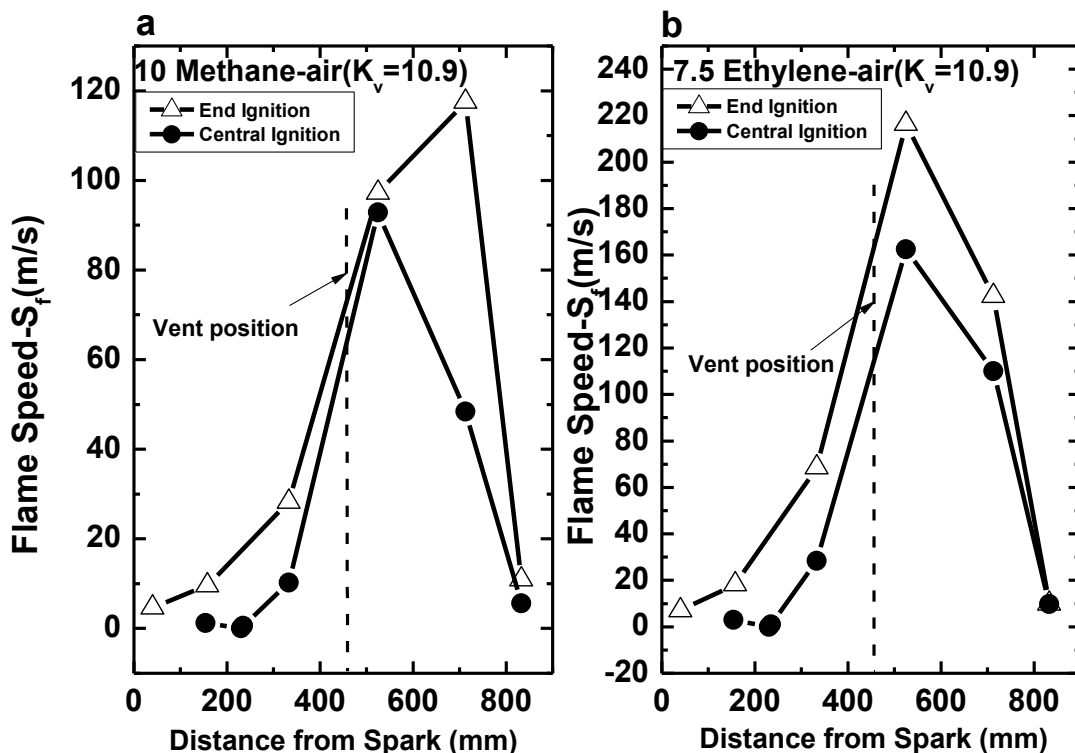


Figure 10: Comparing flame speeds of Centre and End Ignition for  $K_v = 10.9$   
(a) 10% methane-air (b) 7.5% Ethylene-air

## Conclusions

The result from this work for central ignition in a  $0.01 \text{ m}^3$  vessel with an L/D of 2.8 was compared with that of Cooper et al. (1986) for a  $0.68 \text{ m}^3$  rectangular vessel with an L/D of 3. The peak overpressures were due to an external flame in both cases and were very similar for the two test facilities.

The ratio of the peak explosion overpressure for end and central ignition was found to vary from 1.5 to 5.2, depending on  $K_v$ , mixture reactivity, and vessel size.  $P_{\text{ext}}$  was the dominant cause of the peak overpressure for  $K_v$  of 5.4 or lower and  $P_{\text{fv}}$  was the dominant cause of the overpressure for  $K_v$  of 10.9.

The results clearly demonstrate that the ignition position relative to the vent is important and that the highest overpressures are not generated by central ignition, which is the basis of the current vent design correlations. There is therefore a clear need to consider the effects of ignition locations in vent design correlations in order to meet the ATEX directive (European Parliament and Council, 1994) requirement for the worst case conditions to be considered.

## Acknowledgements

Bala Fakandu thanks the Nigerian government through the Petroleum Technology Development Fund for a research scholarship.

## References

- Andrews, G.E., Phylaktou, H.N. (2010). *Explosion Safety, In: Handbook of Combustion*. Eds. Lackner, M., Winter, F., Agarwal, A. K. Chapter 15, Wiley-VCH,
- Bartknecht, W. (1993). *Explosionsschutz, Grundlagen und Anwendung*, Springer Verlag.
- Bauwens, C.R., Chaffee, J. and Dorofeev, S. (2010). Effect of Ignition Location, Vent Size and Obstacles on Vented Explosion Overpressure in Propane-Air Mixtures. *Combustion Science and Technology*, 182:11-12, 1915-1932.
- Bradley, D. and Mitcheson, A. (1978). The venting of gaseous explosions in Spherical Vessels I - Theory. *Combustion and Flame* 32, 221-236.
- Burgoyne, J.H. and Newitt, D.M. (1955). Crankcase Explosions in Marine Engines, *Trans.I.Mar.E.* 18, 255-270.
- Cates, A. and Samuels, B. A (1991) Simple Assessment Methodology for Vented Explosions. *Journal of Loss Prev. Process Ind.* Vol. 4 p. 287-296.
- Cooper, M. G., Fairweather, M., and Tite, J. P. (1988). On the mechanisms of pressure generation in vented explosions. *Combustion and Flame*, 65, 1-14.
- Cubbage, P.A. and Simmons, W.A.(1955). An investigation of explosion reliefs for industrial drying ovens. I-Top reliefs in box ovens, London: The Gas Council: Research Communication GC23. 46.

- European Standard EN 14994:2007. (2007). Gas explosion venting protective systems.
- Fakandu, B.M., Kasmani, R.M., Andrews, G.E. and Phylaktou, H.N. (2011). Gas Explosion Venting and Mixture Reactivity. *Proceedings of 23th International Colloquium on the Dynamics of Explosions and Reactive Systems (ICDERS 2011)*, California.
- Fakandu, B.M., Kasmani, R.M., Andrews, G.E. and Phylaktou, H.N. (2012). The Venting of Hydrogen-Air Explosions in an Enclosure with L/D=2.8. Proc. Ninth International Symposium on Hazardous Process Materials and Industrial Explosions ( IX ISHPMIE), Cracow.
- Fakandu, B.M., Yan, Z.X., Phylaktou, H.N. and Andrews, G.E.(2013). The Effect of Vent Area Distribution in Gas Explosion Venting and Turbulent Length Scales on the External Explosion Overpressure. *Proc. of the Seventh International Seminar on Fire and Explosions Hazards (ISFEH7)*, pp.717-726. doi:10.3850/978-981-07-5936-0\_11-05.
- Ferrara G., Di Benedetto A., Salzano E., Russo G. (2006). CFD analysis of gas explosions vented through relief pipes, *Journal of Hazardous Materials*, 137, 654-665.
- Ferrara F., Willacy S.K., Phylaktou H.N., Andrews G.E., Di Benedetto A., Salzano E., Russo G., (2008). Venting of gas explosion through relief ducts: Interaction between Internal and External Explosions, *Journal of Hazardous Materials*, 155, 358-368.
- Harris, G.F.P. and Briscoe P.G. (1967). The venting of pentane vapour-air explosion on a large vessel. *Combustion and Flame*, Volume 11, 329-338.
- Heinrich, H.J. (1966). Sizing pressure-relief vents for the protection of plants with explosion hazard in Chemical industries. *Chem. Ing. Tech.* 38, 1125.
- Kasmani, R; Willacy, S; Phylaktou, HN; Andrews, G.E. (2006). Self accelerating gas flames in large vented explosion volumes that are not accounted for in current vent design correlations. Proc. 2nd International Conference on Safety & Environment in Process Industry, Naples. 2006. *Chemical Engineering Transactions*, Vol. 9, p.245-250.
- Kasmani, R. M. Fakandu, B.M. Kumar, P. Andrews, G. E. Phylaktou, H. N. (2010). Vented Gas Explosions in Small Vessels with an L/D of 2. *Proceedings of the Sixth International Seminar on Fire and Explosions Hazards*, Bradley, D., Makhviladze, G., and Molkov, V., (Eds.), University of Leeds, Leeds, UK (April 11-16, 2010), 2011. pp. 659-670.
- Nagy, J. and Verakis H.C. (1983). *Development and Control of Dust explosions*, Occupational Health and Safety. Marcel Dekker, Inc, New York.
- National Fire Protection Association (NFPA). (2013), *Guide for Venting of Deflagrations NFPA 68*, USA.
- Maisey, H. R. (1965). Gaseous and Dust Explosion Venting. Part 1, *Chemical and Process Engineering*, pp. 527-535.
- Molkov, V. V. (2001). Turbulence Generated During Vented Gaseous Deflagrations and Scaling Issue In Explosion Protection. *ICHEM E Symposium Series*, No. 149, 279-292.
- The European Parliament and the Council, (1994). *The Explosive Atmosphere Directive (ATEX)*, 94/9/EC. Equipment and Protective Systems Intended for Use in Potentially Explosive Atmospheres, 23.3.
- Swift, I. (1989). NFPA 68 guide for venting of deflagrations: what's new and how it affects you. *Journal of Loss Prevention in the Process Industries*, 2, 5-15.
- Sato, K, Tano, S. and Maeda, Y. (2010) Observations of Venting Explosions in a Small Cubic Vessel with Rich Propane-Air Mixtures. Proc. Sixth Int. Sem. on Fire and Explosion Hazards. p.671-682. Research Publications, ISBN 978-981-08-7724-8. doi:10.3850/978-981-08-7724-8\_10-03



- Solberg, D. M., Pappas, J. A. & Skramstad, E. (1981). Experimental explosion of part confined explosion. Analysis of pressure loads, Part 1. Det Norske Veritas Research Division Technical Report no 79-0483.
- Willacy, S.K. Phylaktou, H.N. Andrews, G.E. Ferrara, G. (2007). Stratified propane-air explosion in a duct vented geometry - Effect of concentration, ignition and injection position. *Journal Process Safety and Environment*, 85(B2), 153-161.